ACS Macro Letters

Letter

pubs.acs.org/macroletters

Fluctuation Effects in Symmetric Diblock Copolymer–Homopolymer Ternary Mixtures near the Lamellar–Disorder Transition

Brian M. Habersberger,[†] Timothy M. Gillard,[†] Robert J. Hickey,[‡] Timothy P. Lodge,[†,‡] and Frank S. Bates*[,†]

[†]Department of Chemical Engineering and Materials Science and [‡]Department of Chemistry, University of Minnesota, Minneapolis, Minnesota 55455, United States

Supporting Information

ABSTRACT: We have systematically mapped the phase behavior of a series of symmetric CE/C/E ternary copolymer/homopolymer mixtures, where C is poly(cyclohexylethylene) and E is poly(ethylene), identifying the location in composition of the technologically important bicontinuous microemulsion (BμE) channel as a function of diblock molecular weight. The lamellar-to-disorder transition, characterized by dynamic mechanical spectroscopy, small-angle X-ray scattering, and optical transmission measurements, exhibits increasingly second-order behavior as the BμE state is approached with increasing homopolymer content. Real-space transmission electron microscopy images obtained from rapidly frozen specimens evidence the development of large-scale fluctuating smectic correlations in the disordered state as the order–disorder transition is approached. This discovery provides fresh insights into the unexplained role of fluctuations in the formation of the BμE in ternary mixtures formed from binary blends of homopolymers that display an Ising-like critical point and a symmetric diblock copolymer governed by a weak, fluctuation-induced, first-order phase transition.

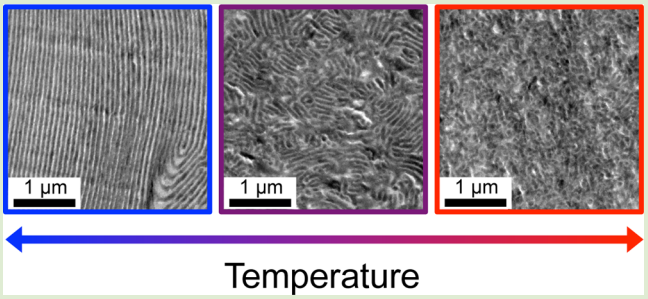

Ternary mixtures of an AB diblock copolymer and the constituent A- and B-type homopolymers, high molecular weight analogues of oil/water/surfactant systems, have been the subject of intense scientific interest due to a combination of practical applications for the materials and interesting problems in fundamental physics encountered in these systems.[1−7] Of primary practical interest is the polymeric bicontinuous microemulsion (BμE). This thermodynamically stable isotropic cocontinuous morphology with tunable domain sizes (50−250 nm) has been exploited as a template to create a variety of other nanoporous functional materials that are of interest for an array of potential applications.[1,2] On a fundamental level, synthetic polymers in general offer remarkable control over the symmetry, length scale, dynamics, and dimensionality of various types of phase transitions making them ideal model systems for studying universal phenomena in condensed matter.[8,9] Specifically, AB/A/B ternary blends display rich phase behavior connecting the self-assembly of pure diblock copolymers into nanoscopically ordered mesophases to macrophase separation of binary homopolymer blends.[5,10]

Symmetric AB diblock copolymers exhibit a fluctuation-induced weakly first-order phase transition of the Brazovskii class between ordered striped (lamellar) and disordered states, where the degree of polymerization (N_{AB}) dictates the fundamental periodic length scale d.[11−15] The domain spacing, $d = 2\pi/q^*$, can be measured by scattering experiments where q^* is the principal (first-order) Bragg reflection. Adding equal amounts of A and B homopolymers ($N_A \approx N_B$) to a symmetric AB diblock copolymer dilates (swells) the lamellae.[2] Within the context of mean-field theory $d \to \infty$ as $\phi_H \to \phi_{H,U}$, where ϕ_H is the total volume fraction of homopolymers and $\phi_{H,U}$ is the unbinding composition, roughly coincident with a predicted higher-order multicritical Lifshitz (L) point (i.e., $\phi_{H,U} \approx \phi_{H,L} = 1/(1 + 2N_AN_B/N_{AB}^2)$).[2,3,10] Experiments have shown that this divergence in periodicity is interrupted by the formation of a finite scale and technologically important BμE in a small window of blend composition.[2] A different universality class, macroscopic phase separation and Ising-like critical behavior characteristic of binary blends, is accessed at higher homopolymer content, $\phi_{H,L} < \phi_H \leq 1$.[3,16] Fluctuations impact each region of this ternary phase diagram differently.[2,4,5,11,16−20] To date, most research on this topic has focused on understanding and exploiting the BμE morphology and characterizing the critical behavior on the homopolymer-rich side of the BμE channel. Less well studied is the lamellar-to-disordered transition on the diblock-rich side of the phase diagram, which is generally assumed to belong to the Brazovskii class, analogous to pure diblocks.[3−5,16,21] Application of the Gibbs phase rule anticipates that, in general, a 2-phase window should separate the ordered and disordered states with varying

Received: August 27, 2014
Accepted: September 28, 2014
Published: October 1, 2014

temperature,[2] although this does not preclude the possibility of a line of continuous (second-order) transitions as a function of ϕ_H as predicted by mean-field theory.[10] In this Letter, we explore the effect of fluctuations on the lamellar-to-disorder (LAM−DIS) phase transition in AB/A/B ternary polymer blends at compositions between the pure diblock copolymer and the onset of the BμE channel.

We have investigated the volumetrically symmetric isopleths of ternary blends that bridge the divide in parameter space between lamellar forming symmetric diblocks and binary homopolymer blends that display upper critical solution temperature behavior. These blends were studied in mixtures of nearly equal amounts by volume of poly(cyclohexylethylene) (C) and polyethylene (E) homopolymers (N_C = 40 and N_E = 37 are the number-average degrees of polymerization based on a 118 Å^3 reference volume) and volumetrically symmetric poly(cyclohexylethylene-*b*-ethylene) (CE) diblock copolymers (f_c = 0.51 ± 0.1; where f_c is the volume fraction of the C block) of various N_{CE}, corresponding to number-average molecular weights M_n = 13, 14, 19, and 38 kg/mol (N_{CE} values of 220, 230, 310, and 630, respectively). These samples are referred to as 13CE, 14CE, 19CE, and 38CE, respectively. All polymers were synthesized and characterized using established methods resulting in narrow molecular weight distributions ($Đ$ < 1.1 in all cases).[22] Experimental and molecular characterization details are summarized in the Supporting Information.

The phase diagram for binary blends of C and E is shown in Figure 1. The boundary between a single-phase and a two-phase region, the binodal curve, was determined from cloud point measurements on slow cooling. This phase diagram has been modeled using Flory−Huggins theory with a composition-dependent segment−segment interaction parameter, $\chi(T, \phi_E) = (\alpha/T - \beta)(1 + c(1 - \phi_E))$, where α, β, and c are constants, resulting in a critical temperature and composition of 260 °C and $\phi_{E,c}$ = 0.37, respectively.[7,23]

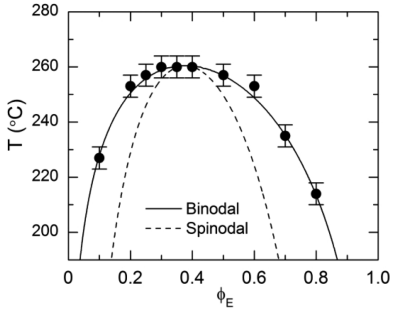

Figure 1. Binary phase diagram for C/E homopolymer blends. Experimentally determined cloud point measurements are represented as black symbols. The binodal and spinodal curves are results of a fit to the data using Flory−Huggins theory with a composition-dependent χ parameter.

In all CE/C/E ternary blends studied here, the volume ratio between the C and E homopolymers was kept constant (ϕ_C/ϕ_E = 1), and the overall total homopolymer volume fraction (ϕ_H = ϕ_C + ϕ_E) was varied. Due to the slight asymmetry of the C/E binary system, the ϕ_E = 0.5 blend at the pure homopolymer end of this isopleth (binodal temperature of 257 °C) is not precisely at the critical composition; this has a trivial impact on the phase behavior as $\phi_H \rightarrow \phi_{H,B\mu E}$. Each blend is referred to as *xx*CE*yy*, where *xx*CE is the CE diblock used in the blend and *yy* is the total homopolymer volume percent.

The ternary CE/C/E phase diagrams along the volumetrically symmetric isopleth are summarized in Figure 2. These

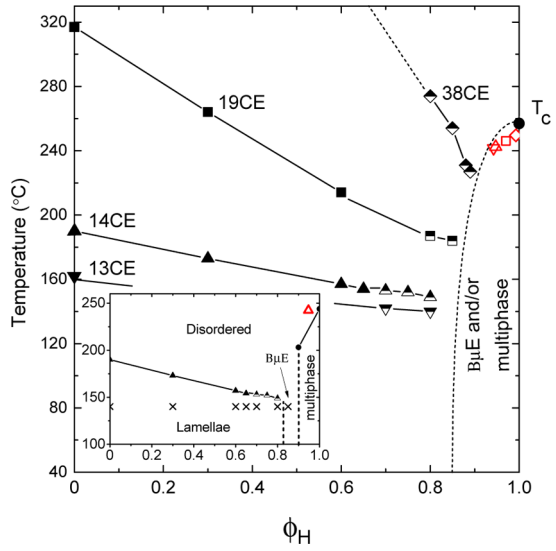

Figure 2. Phase diagrams showing the LAM−DIS transitions along the volumetrically symmetric isopleths for ternary CE/C/E blends with several CE diblocks where ϕ_H represents the total volume fraction of homopolymer. Half-filled symbols indicate blends for which a local minimum of optical transmission was observed at the ODT. T_C is the experimentally determined cloud point for the ϕ_E = 0.5 binary blend from Figure 1. The inset graph is a detailed ternary phase diagram for 14CE containing blends. The cross mark symbols indicate points where SAXS data were collected to determine phase symmetry (see Figure S1, Supporting Information). Empty red symbols indicate predicted Lifshitz composition and temperature. All lines connecting data points are to guide the eye.

were experimentally determined using a combination of optical transmission and dynamic mechanical spectroscopy (DMS) to locate order−disorder transition temperatures (T_{ODT}) and both small-angle X-ray scattering (SAXS) and TEM to determine phase symmetries. In all cases, the low temperature ordered phase is lamellar (LAM). See Figure S1 in the Supporting Information for detailed SAXS patterns. When the C and E homopolymers are blended with the CE diblocks, the homopolymers swell the LAM domains, and the T_{ODT} of the LAM−DIS transition decreases as ϕ_H increases. At high ϕ_H the line of order−disorder transitions (ODTs) terminates at the narrow BμE channel, while a multiphase region characterizes still higher homopolymer contents as ϕ_H approaches 1. As the diblock molecular weight (N_{CE}) increases, larger quantities of homopolymer are needed to reach the BμE channel, following the trend predicted by the theoretical Lifshitz points (calculated to occur at values of $\phi_{H,L}$ of 0.94, 0.95, 0.97, and 0.99 for the 13CE, 14CE, 19CE, and 38CE systems, respectively). However, the onset of the BμE always occurs at values of ϕ_H lower than the predicted Lifshitz points, consistent with previous observations.[2]

The inset of Figure 2 shows a detailed ternary phase diagram for the blends containing the 14CE diblock copolymer. SAXS measurements confirm that the lamellar morphology persists up to ϕ_H = 0.80, and the BμE forms at ϕ_H = 0.85. For $\phi_H \geq$ 0.90, macroscopic phase separation occurs below the envelope of upper critical solution temperatures (UCSTs) identified by cloud points in optical transmission measurements (see Supporting Information).

dx.doi.org/10.1021/mz500531y | *ACS Macro Lett.* 2014, 3, 1041−1045

In addition to simple cloud points that evidence macroscopic phase separation, two other light scattering phenomena were recorded in optical transmission experiments while heating and cooling the ternary blends through the T_{ODT} of the LAM−DIS transition, as shown in Figure 3. We attribute changes in relative transmission in this temperature range to variations in the fraction of incident light scattered to wider angles than collected at the detector in our experimental measurements.[24−26] For blends with low homopolymer content $\phi_H \leq 0.65$, a small discontinuous increase in the transmission occurs in some samples at the T_{ODT} upon heating through the LAM−DIS transition (or reduction upon cooling through the DIS−LAM transition). This behavior is shown for the 14CE60 blend and the pure 14CE diblock ("blend" 14CE0) in Figure 3. This change in transmission coincides with the T_{ODT} measured with DMS, indicated in Figure 3 by an abrupt decline in the storage modulus (G') as the soft solid response of the LAM phase gives way upon heating to liquid-like behavior. Scattering of visible light from the LAM state has been shown to originate from randomly oriented grains of the locally anisotropic and birefringent striped phase.[24−26] When the material disorders, this source of scattering is extinguished, and an increase in transmission occurs.

For blends with higher homopolymer content, a second, unexpected light scattering phenomenon was discovered as the BμE channel was approached. In these blends, a local minimum in the transmission (corresponding to a maximum in scattered intensity) appears at a temperature that is coincident with the T_{ODT} measured with DMS. This is illustrated for the blends 14CE80 and 19CE85 in Figure 3. All blends in which this local minimum in transmission was recorded are shown with half-filled symbols in the phase diagrams in Figure 2. The depth of the local minimum increases with increasing homopolymer content, beginning at approximately $\phi_H \approx 0.70$, where this feature first becomes evident, and becoming most pronounced at values of ϕ_H nearest the BμE channel. In addition, the breadth in temperature of the local minimum of transmission increases with increasing diblock molecular weight. The local transmission minimum is fully reversible upon heating and cooling through the ODT. The location, depth, and breadth of the local minimum of transmission are essentially independent of the rate of change in temperature; only a small hysteresis in the location in temperature of the minimum transmission, T_{min}, was documented at the highest temperature ramp rates ($\Delta T_{min} \approx 3$ °C for a rate of 1 °C/min). Moreover, near the local minimum, ceasing heating or cooling and holding the temperature constant for extended periods of time does not influence the transmission value. For example, the inset in Figure 3 shows the stability of the transmission near the local minimum at T_{ODT} for the 14CE80 blend. Similarly, the reduced transmission at temperatures near T_{ODT} is essentially independent of thermal history. These results confirm that the reduced transmission at temperatures near T_{ODT} is not a transient phenomenon but a manifestation of equilibrium states near the LAM−DIS transition in these ternary blends.

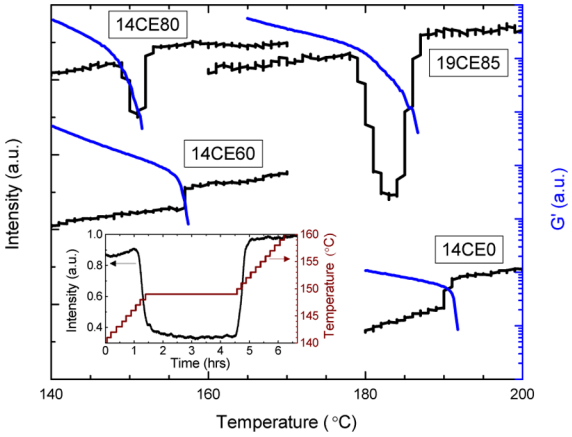

Figure 3. Representative optical transmission and DMS determination of ODT for blends containing 14CE and 19CE polymers. The black and blue lines represent optical transmission and DMS data, respectively. Data were collected while heating at a rate of 1 °C/min. The inset plot shows the time-dependent stability of the transmission for the 14CE80 blend when the heating ramp (at a rate of 0.1 °C/min) was halted at 149 °C, the temperature approximately at the local minimum in transmission. The black and red lines represent the optical transmission and temperature, respectively. Data have been shifted vertically for clarity.

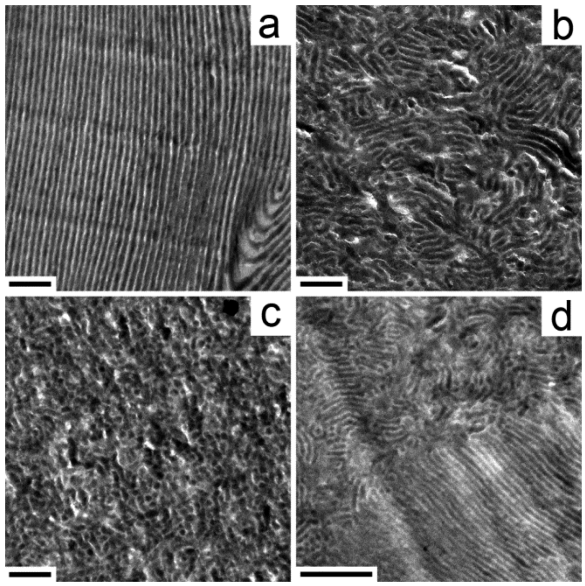

Figure 4. Transmission electron microscopy images depicting the morphology of ternary blends during the LAM−DIS transition. Images represent quenched states after 16 h of annealing (a) below (170 °C), (b) at (230 °C), and (c) above (238 °C) the ODT for sample 38CE88. (d) A coexistence between fluctuating disordered and ordered lamellar phases for sample 19CE85 quenched at 177 °C upon the observation of a reduction in optical transmission during a heating ramp. All scale bars are 500 nm, and samples have been stained with ruthenium tetroxide.

Direct real space imaging by TEM was employed to probe the structure of these materials near the LAM−DIS transition. Because the mixtures solidify near 100 °C (the glass transition for C and the melting transition for E), we were able to freeze and image the morphology at specific temperatures by rapidly immersing the specimen in a dry ice and 2-propanol bath ($T = -78$ °C), which fixes the polymers in less than 5 s. Representative TEM images of the 38CE88 blend near the LAM−DIS transition for samples quenched after annealing for 16 h from temperatures below (Figure 4a), at (Figure 4b), and above (Figure 4c) the local minimum in transmission are shown in Figure 4. These TEM images reveal a well-ordered LAM phase at low temperature (Figure 4a) and an isotropic but

dx.doi.org/10.1021/mz500531y | ACS Macro Lett. 2014, 3, 1041−1045

microphase-separated disordered phase that resembles the BμE at high temperatures at and above the transmission minimum. At 230 °C (Figure 4b), i.e., coincident with the minimum in the optical transmission, the morphology is disordered at large length scales (ca. >1 μm) but characterized by local lamellar (smectic-like) correlations that extend over several hundred nanometers. This strongly fluctuating morphology explains the origins of the loss in light transmission, i.e., a smectic fluctuation correlation length commensurate with the wavelength of visible light. At 238 °C (Figure 4c) the smectic fluctuation correlation length is considerably smaller, consistent with the increase in transmission.

The sharp increase in light scattering near the ODT for homopolymer-rich blends (Figure 3) and the fluctuating morphology evident in Figure 4 lead us to hypothesize that the nature of the LAM−DIS phase transition changes as the BμE channel (and the mean-field predicted Lifshitz point) is approached with increasing homopolymer content. At low homopolymer content ($\phi_H \leq 0.65$), a weakly first-order transition is observed, which we interpret as an extension of the behavior at $\phi_H = 0$ (i.e., pure diblock copolymer) where fluctuations in the local composition at finite q induce the ODT. For $0.65 < \phi_H \leq \phi_{H,B\mu E}$, the LAM−DIS transition is qualitatively different. Here, fluctuations in a second quantity (perhaps related to the interfacial curvature between domain spaces, see below) give rise to the documented smectic correlations of which the characteristic length scale grows as the transition is approached, eventually spanning the sample in the ordered phase. This diverging length scale suggests the system is at or near a continuous second-order LAM−DIS transition. In addition, the reported local minimum in transmission is reminiscent of critical opalescence near a second-order transition.[27] The reported change in character of the LAM−DIS transition for $\phi_{H,L} \leq \phi_H$ may reflect a crossover effect analogous to the crossover between Ising and Lifshitz behavior near the line of critical points in the homopolymer-rich region of the phase diagram ($\phi_{H,L} < \phi_H \leq 1$).[16]

Other experiments at temperatures coincident with the minimum in light transmission suggest that the mixtures reported in Figure 3 may not be located precisely along a line of continuous second-order transitions. For example, Figure 4d shows a TEM image obtained from blend 19CE85 after quenching (during heating at 1 °C/min) from the temperature where the local minimum in transmission occurs. This micrograph shows coexistence between the LAM and disordered phases; smectic-like fluctuations in the disordered state closely resemble those found in Figure 4b. In this case, development of large-scale smectic fluctuations (which should diverge in length scale at a true second-order transition) appears to be cut off by a first-order transition. In practice, verifying the existence of a line of critical points as the BμE is approached requires finely tuning the ratio ϕ_C/ϕ_E at constant ϕ_{CE}, which will be undertaken in future experiments.

The transition from first- to second-order-like behavior in the work presented here is reminiscent of the seminal work by McMillan, in which, using a mean-field treatment, a change from a second- to a first-order transition was predicted for the smectic-A-to-nematic transition in liquid-crystalline molecules with increasing alkyl-chain length due to a coupling of the nematic and smectic order parameters.[28] Here we note that these one-component liquid crystals lack the thermodynamic degrees of freedom necessary to produce multiple phase windows as a function of temperature. The behavior of the CE/C/E ternary blends described in this Letter raises the intriguing possibility of the existence of an additional order parameter, perhaps relating to curvature of the interface dividing the C- and E-rich domains, even in the limit $\phi_H \to 0$. In pure (single component) symmetric diblock copolymers the fluctuating disordered state has been shown to transition to the LAM phase without changing either d or the local composition profile.[12] Attaining constant negative Gauss and zero-mean curvature at the interface dividing the fluctuating domain spaces in the disordered bicontinuous morphology (a general driving force in self-assembled soft materials governed by constant density)[29] requires twisting the saddle-shaped interfacial surface, introducing the possibility of local chirality in the system (similar geometric arguments result in the familiar gyroid phase).[30,31] Adding homopolymer alleviates such packing constraints (since the homopolymers are not pinned to the interface), perhaps altering this hypothetical order parameter and facilitating the development of smectic fluctuations with arbitrary correlation length without the need to twist the local interfacial surface topology.

In the $\phi_H \to 0$ (and $\phi_H \to 1$) limit, as $N_{AB} \to \infty$ ($N_A = N_B \to \infty$) and $d \to \infty$ (and the correlation length $\xi \to \infty$),[32,33] the effects of fluctuations disappear leading to the recovery of a (mean-field) second-order ODT (and mean-field versus Ising-like critical scaling exponents). By analogy, as $\phi_H \to \phi_{H,U}$ and $d \to \infty$ we might expect the symmetric ternary mixture to become more mean-field-like. Theory anticipates that a (mean-field) multicritical Lifshitz point occurs when $N_{AB} \to \infty$ and $N_A = N_B \to \infty$ at finite N_{AB}/N_A. However, the greater upper and lower critical dimensions associated with the Lifshitz point[34] make the symmetric ternary mixture more susceptible to fluctuation effects than the binary homopolymer blend; the upper critical dimension for the undiluted symmetric diblock copolymer appears to be infinite.[35] The added degrees of freedom associated with 3 components, and the mixing of universality classes, leads to the formation of an entirely different phase state, a bicontinuous microemulsion as $d \to \infty$. We believe the experimental evidence presented here offers clues regarding the underlying competition between fluctuation effects in the LAM and DIS phases and the transition to the fascinating bicontinuous microemulsion, which has not yet been described by fundamental theory.

The ability to precisely tune the molecular (e.g., N_{AB}, $N_A = N_B$) and thermodynamic (T_{ODT}, T_c, and ϕ_H) parameters, along with access to quantitative real-space and reciprocal-space structural probes, makes AB/A/B mixtures especially attractive as model systems for studying the universal behavior of condensed matter systems, in particular one-dimensionally ordered lamellar or striped phases.[36−38] Striped phases govern the physical properties of a host of condensed matter systems including high-temperature superconductors,[39−41] magnetic alloys,[42] and liquid crystals.[43] For example, the fluctuating smectic correlations reported here are perhaps analogous to recent work where fluctuating charge stripes were observed near the charge order temperature for high-temperature superconducting cuprates.[40] Understanding the universal phase behavior that governs this form of one-dimensional order is complicated by difficulties associated with precisely tuning the interactions that give rise to striped phases, along with visualizing fluctuations, which generally dominate the transition from disorder to a state of one-dimensional order. Ternary blends of symmetric AB diblock copolymers and the

associated A and B homopolymers provide an ideal remedy to these problems.

■ ASSOCIATED CONTENT

Supporting Information

Detailed experimental procedures, polymer characterization, X-ray scattering data, optical transmission schematic, and additional TEM images. This material is available free of charge via the Internet at http://pubs.acs.org.

■ AUTHOR INFORMATION

Corresponding Author

*E-mail: bates001@umn.edu.

Notes

The authors declare no competing financial interest.

■ ACKNOWLEDGMENTS

This research was supported by the National Science Foundation under award DMR-1104368. Portions of this work were performed at the DuPont-Northwestern-Dow Collaborative Access Team (DND-CAT) located at Sector 5 of the Advanced Photon Source (APS). DND-CAT is supported by E.I. DuPont de Nemours & Co., The Dow Chemical Company and Northwestern University. Use of the APS, an Office of Science User Facility operated for the U.S. Department of Energy (DOE) Office of Science by Argonne National Laboratory, was supported by the U.S. DOE under Contract No. DE-AC02-06CH11357. Parts of this work were carried out in the Characterization Facility, University of Minnesota, which receives partial support from NSF through the MRSEC program.

■ REFERENCES

(1) Jones, B. H.; Lodge, T. P. *Polym. J.* **2012**, *44*, 131−146.
(2) Bates, F. S.; Maurer, W. W.; Lipic, P. M.; Hillmyer, M. A.; Almdal, K.; Mortensen, K.; Fredrickson, G. H.; Lodge, T. P. *Phys. Rev. Lett.* **1997**, *79*, 849−852.
(3) Schwahn, D.; Mortensen, K.; Frielinghaus, H.; Almdal, K. *Phys. Rev. Lett.* **1999**, *82*, 5056−5059.
(4) Schwahn, D.; Mortensen, K.; Frielinghaus, H.; Almdal, K.; Kielhorn, L. *J. Chem. Phys.* **2000**, *112*, 5454−5472.
(5) Pipich, V.; Schwahn, D.; Willner, L. *J. Chem. Phys.* **2005**, *123*, 124904.
(6) Hillmyer, M. A.; Maurer, W. W.; Lodge, T. P.; Bates, F. S.; Almdal, K. *J. Phys. Chem. B* **1999**, *103*, 4814−4824.
(7) Washburn, N. R.; Lodge, T. P.; Bates, F. S. *J. Phys. Chem. B* **2000**, *104*, 6987−6997.
(8) Bates, F. S. *Science* **1991**, *251*, 898−905.
(9) Chaikin, P. M.; Lubensky, T. C. *Principles of Condensed Matter Physics*; Cambridge University Press: Cambridge, England, 2000.
(10) Broseta, D.; Fredrickson, G. H. *J. Chem. Phys.* **1990**, *93*, 2927−2938.
(11) Fredrickson, G. H.; Helfand, E. *J. Chem. Phys.* **1987**, *87*, 697−705.
(12) Lee, S.; Gillard, T. M.; Bates, F. S. *AIChE J.* **2013**, *59*, 3502−3513.
(13) Voronov, V. P.; Buleiko, V. M.; Podneks, V. E.; Hamley, I. W.; Fairclough, J. P. A.; Ryan, A. J.; Mai, S. M.; Liao, B. X.; Booth, C. *Macromolecules* **1997**, *30*, 6674−6676.
(14) Rosedale, J. H.; Bates, F. S.; Almdal, K.; Mortensen, K.; Wignall, G. D. *Macromolecules* **1995**, *28*, 1429−1443.
(15) Brazovskii, S. A. *Sov. Phys. JETP* **1975**, *41*, 85−89.
(16) Schwahn, D. *Adv. Polym. Sci.* **2005**, *183*, 1−61.
(17) Bates, F. S.; Rosedale, J. H.; Fredrickson, G. H. *J. Chem. Phys.* **1990**, *92*, 6255−6270.
(18) de Gennes, P. G. *J. Chem. Phys.* **1980**, *72*, 4756−4763.
(19) Düchs, D.; Ganesan, V.; Fredrickson, G. H.; Schmid, F. *Macromolecules* **2003**, *36*, 9237−9248.
(20) Bates, F. S.; Rosedale, J. H.; Stepanek, P.; Lodge, T. P.; Wiltzius, P.; Fredrickson, G. H.; Hjelm, R. P. *Phys. Rev. Lett.* **1990**, *65*, 1893−1896.
(21) Pandav, G.; Ganesan, V. *Macromolecules* **2013**, *46*, 8334−8344.
(22) Cochran, E. W.; Bates, F. S. *Macromolecules* **2002**, *35*, 7368−7374.
(23) Qian, C.; Mumby, S. J.; Eichinger, B. E. *Macromolecules* **1991**, *24*, 1655−1661.
(24) Balsara, N. P.; Garetz, B. A.; Dai, H. J. *Macromolecules* **1992**, *25*, 6072−6074.
(25) Balsara, N. P.; Perahia, D.; Safinya, C. R.; Tirrell, M.; Lodge, T. P. *Macromolecules* **1992**, *25*, 3896−3901.
(26) Garetz, B. A.; Newstein, M. C.; Dai, H. J.; Jonnalagadda, S. V.; Balsara, N. P. *Macromolecules* **1993**, *26*, 3151−3155.
(27) Stanley, H. E. *Introduction to Phase Transitions and Critical Phenomena*; Oxford University Press: New York, 1971.
(28) McMillan, W. L. *Phys. Rev. A* **1971**, *4*, 1238−1246.
(29) Seddon, J. M. *Biochim. Biophys. Acta* **1990**, *1031*, 1−69.
(30) Fogden, A.; Hyde, S. T. *Eur. Phys. J. B* **1999**, *7*, 91−104.
(31) Matsen, M. W.; Bates, F. S. *J. Chem. Phys.* **1997**, *106*, 2436−2448.
(32) Leibler, L. *Macromolecules* **1980**, *13*, 1602−1617.
(33) de Gennes, P. G. *Scaling Concepts in Polymer Physics*; Cornell University Press: Ithica, NY, 1979.
(34) Bates, F. S.; Maurer, W.; Lodge, T. P.; Schulz, M. F.; Matsen, M. W.; Almdal, K.; Mortensen, K. *Phys. Rev. Lett.* **1995**, *75*, 4429−4432.
(35) Glenn Fredrickson, personal communication.
(36) Seul, M.; Monar, L. R.; O'Gorman, L.; Wolfe, R. *Science* **1991**, *254*, 1616−1618.
(37) Seul, M.; Andelman, D. *Science* **1995**, *267*, 476−483.
(38) Malescio, G.; Pellicane, G. *Nat. Mater.* **2003**, *2*, 97−100.
(39) Kivelson, S. A.; Bindloss, I. P.; Fradkin, E.; Oganesyan, V.; Tranquada, J. M.; Kapitulnik, A.; Howald, C. *Rev. Mod. Phys.* **2003**, *75*, 1201−1241.
(40) Abeykoon, A. M. M.; Božin, E. S.; Yin, W.-G.; Gu, G.; Hill, J. P.; Tranquada, J. M.; Billinge, S. J. L. *Phys. Rev. Lett.* **2013**, *111*, 096404.
(41) Valla, T.; Fedorov, A. V.; Lee, J.; Davis, J. C.; Gu, G. D. *Science* **2006**, *314*, 1914−1916.
(42) Zhao, J.; Shen, Y.; Birgeneau, R. J.; Gao, M.; Lu, Z.-Y.; Lee, D. H.; Lu, X. Z.; Xiang, H. J.; Abernathy, D. L.; Zhao, Y. *Phys. Rev. Lett.* **2014**, *112*, 177002.
(43) Link, D. R.; Natale, G.; Shao, R.; Maclennan, J. E.; Clark, N. A.; Körblova, E.; Walba, D. M. *Science* **1997**, *278*, 1924−1927.